Characterization of modulation structure in $La_2CuO_{4.12}$ by electron diffraction

M. Gao
Beijing Laboratory of Electron Microscopy, Institute of Physics and Center for Condensed Matter Physics, Chinese Academy of Sciences, 100080 Beijing, China

G. D. Liu, G. C. Che, and Z. X. Zhao
National Laboratory for Superconductivity, Institute of Physics and Center for Condensed Matter Physics, Chinese Academy of Sciences, 100080 Beijing, China

L.-M. Peng*
Beijing Laboratory of Electron Microscopy, Institute of Physics and Center for Condensed Matter Physics, Chinese Academy of Sciences, 100080 Beijing, China
and Department of Electronics, Peking University, Beijing 100087, China
(Received 17 July 2000; revised manuscript received 5 February 2001; published 26 November 2001)

The technique of electron diffraction has been used for characterizing the modulation structure in a heavily oxygenated $La_2CuO_{4.12}$ sample. Ordering with modulation directions in bc and ab plane was observed, and the strong dependence of the bc plane ordering on temperature and doping level was established. It was found that low temperature and high doping level enhance the ordering and favor a longer modulation period than otherwise. In some regions, a kind of modulation along c axis has also been found and concluded to be an indication of the staging behavior of the interstitial oxygen ions.

DOI: 10.1103/PhysRevB.64.224113 PACS number(s): 61.72.−y, 61.14.Lj, 82.80.Pv

I. INTRODUCTION

Oxygen-doped $La_2CuO_{4+\delta}$ is one of the simplest systems in the family of high temperature superconducting Cu oxides. Many interesting physical phenomena closely related to the mechanism of high-T_c superconductivity have been found in this simple system, and most of them have not been rationally understood. The complexity associated with this system is caused mainly by the high mobility of the intercalated oxygen ions. The insulating parent compound La_2CuO_4 may be transformed into superconducting phases via hole doping either by adding excess oxygen ions or by adding alkaline earth ions (Sr^{2+}, Ba^{2+}, or Ca^{2+}) which replace La^{3+} of the parent compound. The alkaline earth ions become immobile at relatively high temperatures, while the oxygen atoms (which were determined to occupy the interstitial sites between adjacent LaO layers) remain mobile even below room temperature. One associated phenomenon is the well studied phase separation phenomenon in which the doped holes and intercalated oxygen ions tend to form domains of different densities for $0.01 \leqslant \delta \leqslant 0.055$.[1–6] Jorgensen and co-workers have carried out extensive studies on $La_2CuO_{4+\delta}$ and concluded that the superconducting compound resulted from phase separation near room temperature into two quasi-isostructural orthorhombic phases. The oxygen content of the superconducting phase (with *Fmmm* space group) was estimated to be $\delta \approx 0.08$; while that of the antiferromagnetic insulating phase (*Bmab*) had $\delta \approx 0.7$.[7–9] In addition, the excess oxygen atoms were found to be located between the two LaO layers, and to be tetrahedrally coordinated to four La atoms.[10,11] In hole rich domains the holes exhibit certain degree of ordering which is also known as stripe phase, and this is regarded by some researchers as a promising clue for understanding high temperature superconductivity.[12–17] According to Emery *et al.*,[12,13] a stripe phase is one in which the doped charges are concentrated along spontaneously generated domain walls separating antiferromagnetic insulating regions. The stripes are generated by the competition between the clustering tendency of the holes and the long-range Coulomb interactions. Experimentally, evidence for stripe phases in doped antiferromagnets comes mainly from neutron scattering,[12] and also from many other methods which are capable of probing the local atomic and electronic structure such as nuclear magnetic resonance (NMR),[18,19] extended x-ray absorption fine structure (EXAFS),[20–22] x-ray diffraction,[23] angle-resolved photoemission spectroscopy (ARPES),[24] and electron diffraction.[25–27] However, the concept of stripe phase is still elusive, because the stripe phase is dynamical and instantaneous by nature which prevented it from being studied in details by most high resolution techniques. The static stripe phases may sometimes be observed, but mainly in samples with depressed superconductivity.[14] The distribution of the doped oxygen ions is also an important aspect for understanding the electronic and magnetic behaviors of $La_2CuO_{4+\delta}$. $La_2CuO_{4+\delta}$ ($0.01 \leqslant \delta \leqslant 0.055$) with mobile excess oxygen atoms has a tendency to phase separate into oxygen-rich (hole-rich and superconducting) and oxygen-poor (hole-poor and antiferromagnetic) phases.[1–6] Furthermore, the staging behavior of the excess oxygen in $La_2CuO_{4+\delta}$ and its nonsuperconducting analog $La_2NiO_{4+\delta}$ has been demonstrated by neutron diffraction, i.e., the doped oxygen ions tend to form ordered structures along c axis.[15,28–32]

While the technique of electron diffraction is generally very sensitive to charge-density modulations and the associated atomic displacement patterns,[33,34] this technique has not been very successful in the studies of stripe phases and the

ordering of the interstitial oxygen ions. In fact, a few electron diffraction studies have been carried out for $La_2CuO_{4+\delta}$ (Refs. 35,36) and $La_2NiO_{4+\delta}$,[37–39] and modulation structures have been reported. Generally, the modulation was attributed to the ordering of the interstitial oxygen. However, these reports were not consistent with the recent results of neutron diffraction. In particular no modulation along *c* axis has so far been observed by electron diffraction. In a previous study, we have carried out a detailed study on the modulation structure occurring in a heavily Cu-doped and phase separated $La_2CuO_{4+\delta}$ sample.[40,41] The modulation structure found in our system was very similar to those observed previously,[35,36] but the observed modulation exhibited an inverse doping dependence compared with the interstitial oxygen ordering. By using electron energy loss spectroscopy (EELS) as a spatially resolved probe for measuring the local hole density, we found that the modulation period decreased when local hole density was reduced. This characteristic of density dependence was similar to the charge ordering found in $La_{2-x}Sr_xNiO_4$ by Chen *et al.* using electron diffraction.[25]

In this study, electron diffraction was used to study the modulation structure occurring in $La_2CuO_{4+\delta}$. The dependence of the modulation on the temperature and on the doping density is important to determine the nature of the modulation. However, in oxygen-doped $La_2CuO_{4+\delta}$, it is difficult to quantitatively control the excess oxygen and to determine the local densities of the excess oxygen and the hole. We have shown that the electron irradiation may decrease the local hole density by probably reducing the amount of interstitial oxygen atoms,[41] so in this study, we chose a heavily oxygen doped $La_2CuO_{4+\delta}$ sample and the effect of the electron irradiation on the modulation structure was investigated. To certain degree our results may be regarded to reflect the doping dependence of the modulation structure.

II. EXPERIMENT

Insulating La_2CuO_4 compounds were synthesized by the standard ceramic method from the corresponding oxides with purity higher than 99.9%. Oxygen intercalation onto the material was achieved using the method of Takayama-Mouromachi *et al.*[42] The excess oxygen content δ was determined to be 0.12 referring to the data given in Ref. 36. Superconducting property measurements by a MPMS-5 SQUID magnetometer under an applied field of 10 G indicated that this sample contained two superconducting phases, with superconducting temperatures of 15 K (36.9%) and 41 K (63.1%) respectively. This result further supports our estimation that the oxygen content ~ 0.12.[43]

Transmission electron microscopy (TEM) observations were carried out using a Philips CM200 field emission gun (FEG) TEM equipped with a Gatan imaging filter (GIF). The operating voltage used was 200 keV. A Gatan liquid nitrogen double-tilt cooling stage which is capable of varying the sample temperature between 93 K and 373 K was employed for low temperature experiments. $La_2CuO_{4.12}$ powder was crushed in ethanol and the resulting suspension was deposited onto a TEM grid covered with a holy carbon film. The grid was then quickly transferred into the TEM for observations. Lagueyte *et al.*[36] noted that it was difficult to study the superstructure because the satellite reflections were always very weak. In this study, we used the high quality slow-scan CCD camera of the GIF system which allows real-time examinations of diffraction patterns. Weak superlattice reflections may therefore be identified much more easily by adjusting the contrast and brightness of the digitally recorded electron diffraction patterns.

III. RESULTS AND DISCUSSIONS

A. *bc*-plane modulation structure

It should be pointed out that heavy oxidation introduces high density of {110} twins into most grains of polycrystalline $La_2CuO_{4+\delta}$ samples. But the *a* and *b* lattice parameters in orthorhombic $La_2CuO_{4+\delta}$ phases differ only slightly. In selected-area electron diffraction (SAED) patterns $(h0l)$ and $(0kl)$ $(h=k)$ reflections superimpose and it is not possible and necessary to make distinction between [100] and [010] zone axes.

Along principal [100], [110], [130], and [001] zone axes, superlattice reflections were observed at both room temperature (RT$\sim$300 K) and 100 K. We found that along those principal zone axes which are normal to the *c* axis, the observed satellite reflections are very similar to those reported previously.[35,36,41] Figs. 1(a), 2(a), and 2(b) show SAED patterns obtained from [100], [110], and [130] zone axes at 100 K, respectively. Superlattice reflections resulting from superstructure may be seen clearly around the main Bragg reflections in these patterns. In fact, the geometry of the superlattice diffraction pattern is very complex, and multiple superlattice wave vectors coexisted in the pattern. We noted, however, that the diffraction pattern is usually dominated by one set of superlattice reflections which may be described by one wave vector. Generally, the superstructure reflections can be written in the form $\mathbf{G}\pm m\mathbf{q}$, where $\mathbf{G}$ corresponds to the strong main Bragg reflection, m is an integer, $\mathbf{q}=h'\mathbf{a}^*+k'\mathbf{b}^*+l'\mathbf{c}^*$ is the primary modulation vector, and $\mathbf{a}^*$, $\mathbf{b}^*$, and $\mathbf{c}^*$ are the reciprocal lattice unit vectors. In Fig. 1(a), two sets of superlattice reflections can be seen around each fundamental Bragg reflection. The inset in Fig. 1(a) is a schematic drawing depicting the geometry of the SAED pattern. The open circles represent the superlattice reflections expected from a two- or three-dimensional modulation. Figure 1(a) shows that these reflections are either absent or too weak to be observed, we may conclude therefore that the two sets of superlattice reflections come from different domains and the modulation in each single domain is a one dimensional modulation. In Fig. 1(a) it is seen that superlattice reflections are symmetric with respect to the main reflections, i.e., the intensities of $\mathbf{G}+m\mathbf{q}$ and $\mathbf{G}-m\mathbf{q}$ reflections are of the same order, indicating that the direction of the modulation vectors lay approximatively in the *bc* plane. The dominant modulation vector measured from the pattern may be written as $0.18\mathbf{b}^*\pm(0.26\sim0.28)\mathbf{c}^*$ with a modulation period $\sim$25.5 Å, which is near $\mathbf{b}^*/6\pm\mathbf{c}^*/4$ ($\sim$27.6 Å). In [110] and [130] zone axis SAED patterns (Fig. 2), it is noted that the superlattice reflections around the high order main Bragg reflections are stronger than those around the low order ma-

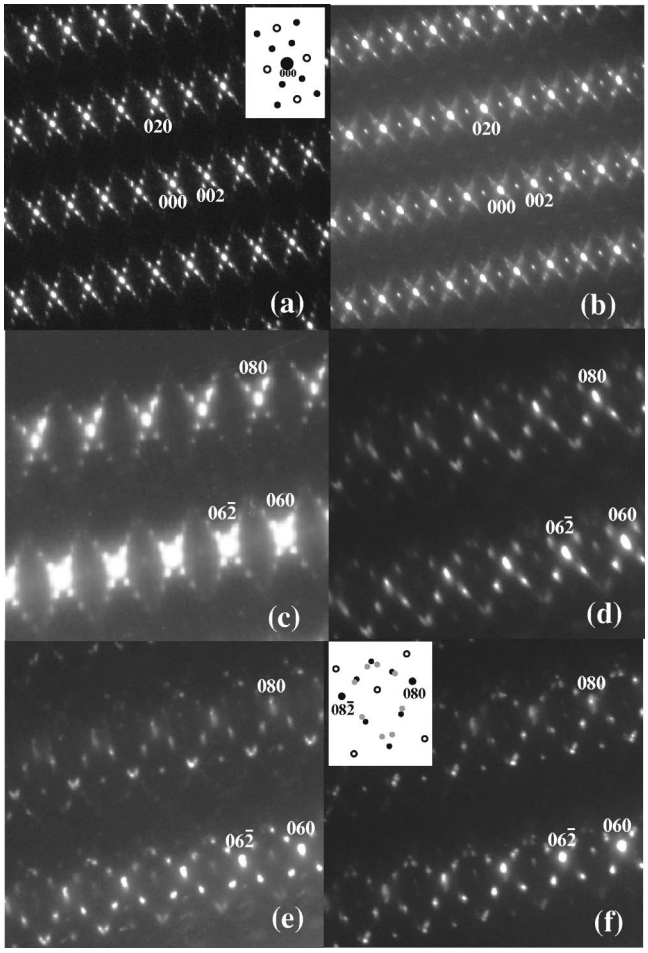

FIG. 1. [100] SAED patterns recorded at 100 K. In (a) and (c) are the center and outer parts of the first recorded diffraction pattern. (b) and (d) are corresponding parts of a diffraction pattern recorded after slight irradiation. (e) and (f) are similar to (c) and (d), but subjected to further irradiation. The insets in (a) and (f) show the geometry of the satellite spots around the matrix reflections. Filled dots represent reflections expected from two domains of one-dimensional modulation, while filled dots plus open circles are those reflections expected from a domain of two-dimensional modulation.

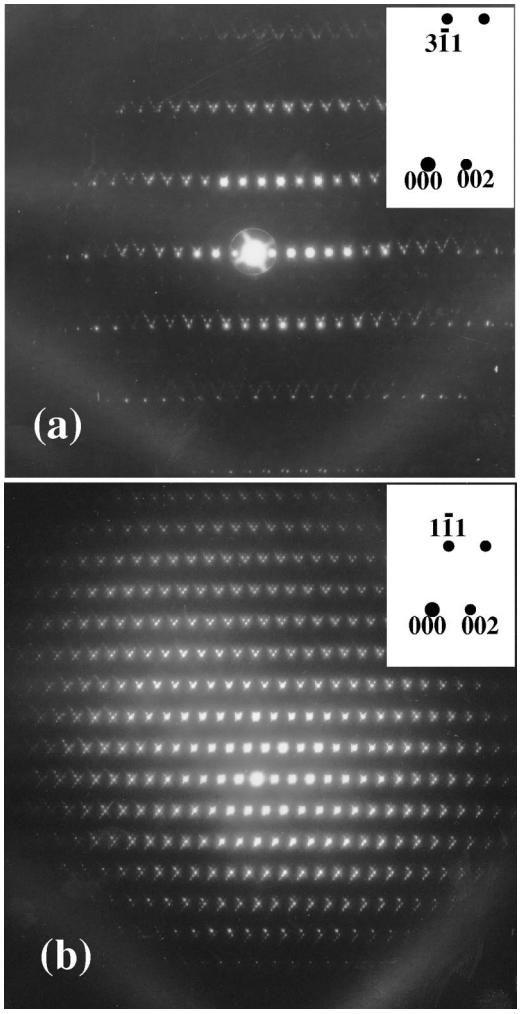

FIG. 2. (a) [110] and (b) [130] SAED patterns recorded at 100 K. Shown in the insets are electron diffraction geometry of a few fundamental reflections around the transmitted zero beam.

trix reflections. In addition, most of the $\mathbf{G}-m\mathbf{q}$ are absent, i.e., superlattice reflections only appear on one side of the main reflections. These features suggest that the reciprocal lattice plane containing the modulation wave vectors is far from the observed reciprocal planes, and the same features have also been found and explained clearly in Cu-doped $La_2CuO_{4+\delta}$.[41] The main point is that there exists a large angle between the reciprocal plane containing matrix reflections and the line containing the one-dimensional modulation vectors. For the main reflections near (000), the superlattice reflections do not intersect with the Ewald sphere. Those around higher order main reflections may, however, intersect with the Ewald sphere, and this is especially so if the superlattice reflections involve only small angles of scattering and if these reflections are elongated as shown in Fig. 3. For some main reflections $\mathbf{G}$, both $\mathbf{G}+\mathbf{q}$ and $\mathbf{G}+2\mathbf{q}$ may be strongly excited. On the other hand, all superlattice reflections of the type $\mathbf{G}-m\mathbf{q}$ lie outside the Ewald sphere and are not appropriately excited. Superlattice reflections therefore only appear on one side of the main spots, and this is illustrated by Fig. 3. From [110] and [130] SAED patterns, the $\mathbf{c}^*$ component of the modulation wave vector is estimated also to be 1/4, the same as that showing in Fig. 1(a). These results suggest that the superlattice reflections observed along different axes normal to c axis at 100 K are projections of a one-dimensional bc-plane modulation reciprocal lattice onto different reciprocal planes.

At room temperature, the observed superlattice reflections were very different from those found at 100 K. First, the intensity of the superlattice reflections were much weaker and were indeed difficult to identify. Second, the dominant vector was always the one with a $\mathbf{c}^*/2$ component. Moreover, the superlattice reflections appearing in the center of Fig. 4(a) turned out to be weaker than those found in the out-region shown in Fig. 4(c). These features indicated that the modulation direction had deviated from the bc plane. Figures 4(a) and 4(b) show two typical [100] and [130] SAED patterns recorded at RT, revealing basically only weak

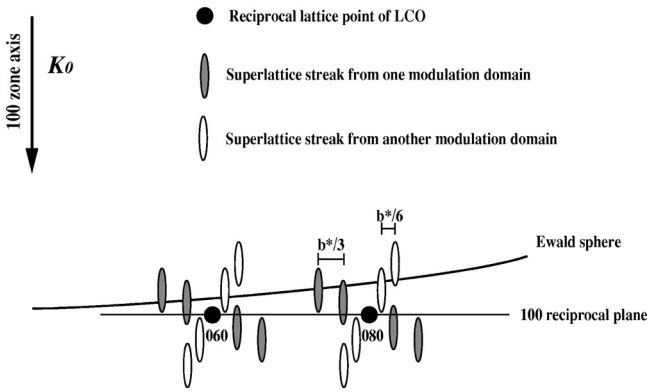

FIG. 3. Schematic diagram showing the generation of the superlattice reflections around high-order main reflections in the outer regions of [100] SAED patterns recorded after irradiation or at high temperature, such as Figs. 1(f) and 5(b).

modulation with $\mathbf{c}^*/2$ component. Figure 4(c) shows the magnified out region of the same [100] SAED pattern as shown in Fig. 4(a) in which some higher order main Bragg reflections are included. Though superlattice reflections appeared on both sides of the main reflections, they were not symmetric with respect to the (010) direction. Similar phenomenon was also observed in the Cu-doped $La_2CuO_{4+\delta}$ sample.[41] Assuming that the two unsymmetric superlattice reflections result from two symmetry related modulation structures due to, e.g., twins, the modulation wave vectors may then be written as $\mathbf{a}^*/6 \pm \mathbf{b}^*/3 \pm \mathbf{c}^*/2$ (with a modulation period ~ 12.7 Å). At RT, the $(00l)$ $(l=2n+1, n=0,1,2,\ldots)$ reflections may be seen clearly. The appearance of these reflections were in contradiction with both the *Bmab* and *Fmmm* space groups so far proposed for $La_2CuO_{4+\delta}$. It is our view that these $(00l)$ reflections are not an independent evidence indicating a modulation along *c* axis, but an adjunct phenomenon resulting from a modulation with a $\mathbf{c}^*/2$ component or the change of space group.

The *bc*-plane modulation structure was unstable upon electron irradiation. Long time irradiation under very weak electron beam at 100 K caused the modulation structure to change. Figure 1(b) shows a [100] SAED pattern recorded from the same sample area as Fig. 1(a) but after two hours very weak electron beam irradiation. The modulation wave vector $0.18\mathbf{b}^* \pm (0.26 \sim 0.28)\mathbf{c}^*$ found in Fig. 1(a) was not the dominant one any more, instead the dominating modulation wave vector became $0.14\mathbf{a}^* \pm 0.27\mathbf{b}^* \pm 0.43\mathbf{c}^*$ (with a modulation period ~ 15.3 Å). This can be seen more easily in Figs. 1(c) and 1(d) which are magnified out regions of Figs. 1(a) and 1(b), respectively. $(00l)$ reflections became visible in Fig. 1(d), suggesting the presence of the modulation with the wave vector $\mathbf{a}^*/6 \pm \mathbf{b}^*/3 \pm \mathbf{c}^*/2$. Figures 1(e) and 1(f) are SAED patterns recorded after further irradiation. These figures show that with increasing electron dose the modulation with $\mathbf{c}^*/2$ component became clearer. In the inset of Fig. 1(f) it is shown a schematic drawing indicating the coexistence of the two sets of modulation vectors, one set is denoted by black dots, while the other set as shadowed dots.

The effect of increasing temperature on the modulation structure is very similar to that of the electron irradiation. In our experiment, the temperature was increased at an interval of 10–20 K, and at each temperature the sample was left in the electron microscope without any electron beam irradiation for 1 h, and the sample was exposed to the electron beam only when recording SAED patterns. In Figs. 5(a)–5(c) we show the SAED patterns recorded at 140, 180, and 220 K, respectively. Intensity profiles were obtained from

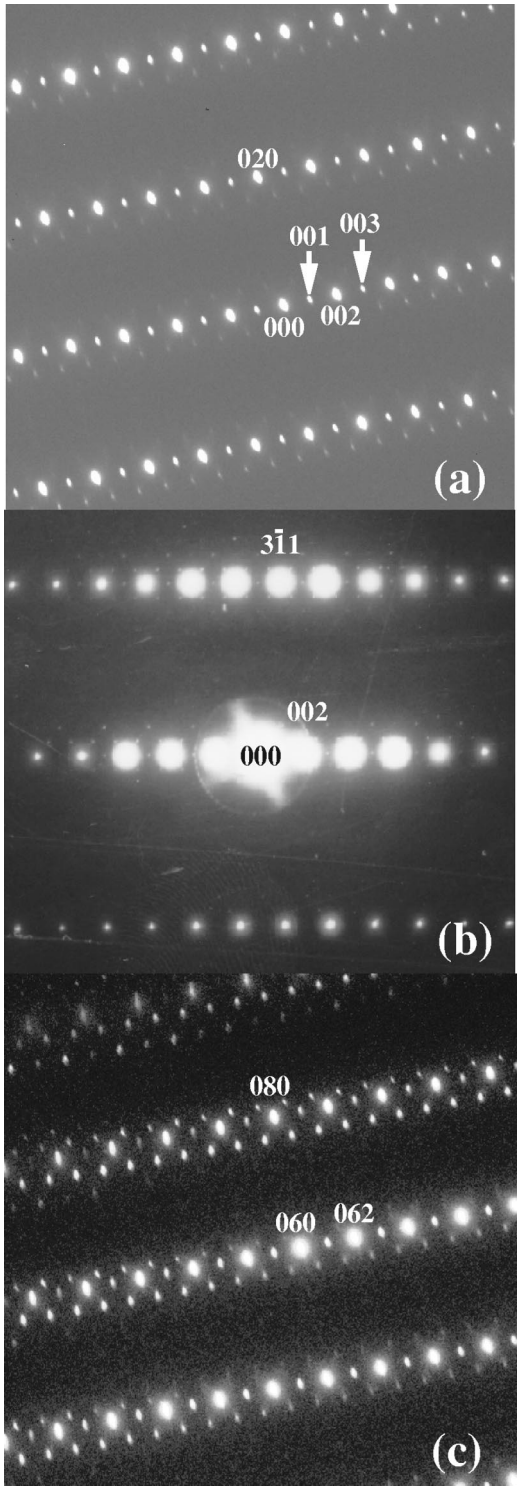

FIG. 4. (a) [100] and (b) [130] SAED pattern recorded at RT, (c) is the outer part of (a).

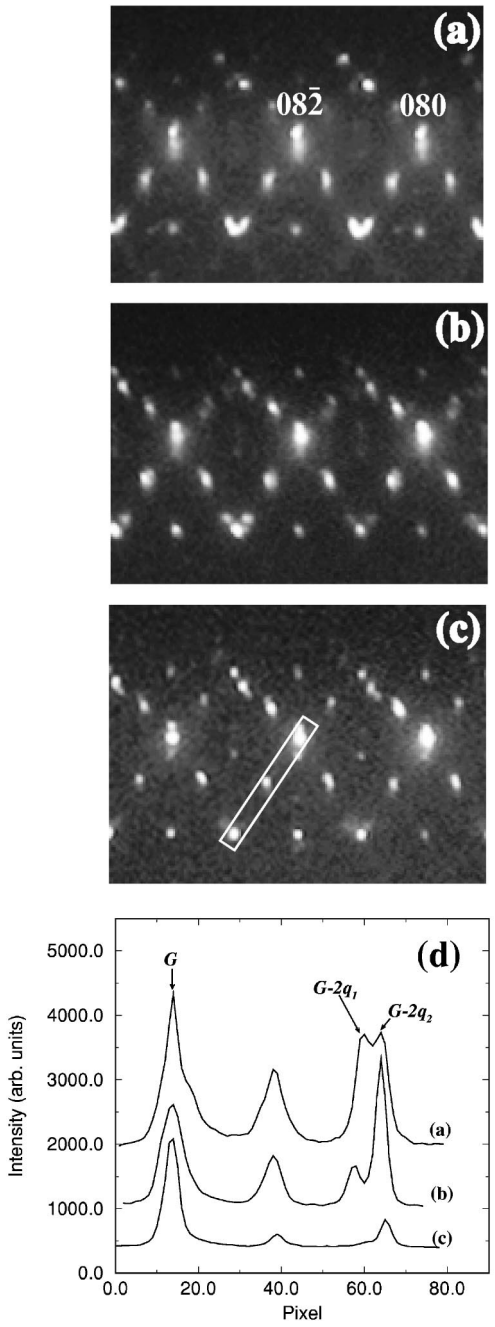

FIG. 5. (a)–(c) Partial SAED patterns recorded at 140, 180, and 220 K. (d) Line scanning result in (a)–(c), and (d) the corresponding intensity profiles obtained from the box as shown in (c). **G** is the main $(08\bar{2})$ reflection, and $\mathbf{q}_1$ and $\mathbf{q}_2$ are $0.14\mathbf{a}^*+0.27\mathbf{b}^*+0.43\mathbf{c}^*$ and $\mathbf{a}^*/6+\mathbf{b}^*/3+\mathbf{c}^*/2$, respectively.

these patterns and the result are shown in Fig. 5(d). As the temperature was increased, the relative intensities of the superlattice reflections described by the wave vector $\mathbf{a}^*/6 \pm \mathbf{b}^*/3 \pm \mathbf{c}^*/2$ became stronger. When the temperature was raised to the range from 150 to 250 K, the wave vector with $\mathbf{c}^*/2$ component became the dominant one. At RT, this wave vector became the only existing one but intensities of the associated superlattice reflections were very weak, all other superlattice reflections associated with different modulation

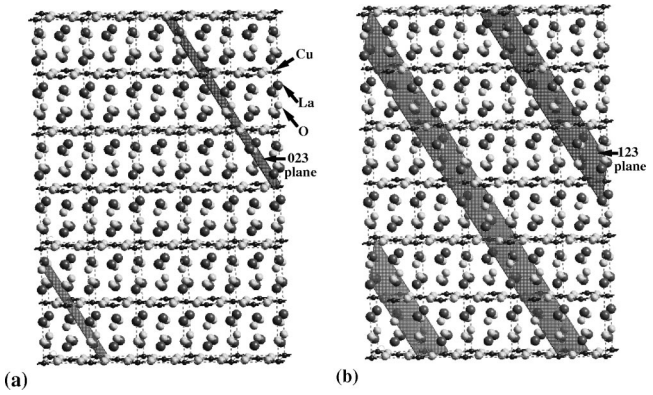

FIG. 6. Real-space schematic diagram showing the modulation structures with a (a) long period and (b) short period. The shadow planes represent charge density modulation planes.

wave vectors disappeared. In addition, we noticed that this transition was not reversible. When the sample was cooled down to ~100 K again, though the intensities of the superlattice reflections were somehow enhanced, the modulation wave vector did not change and remain the same one with a $\mathbf{c}^*/2$ component.

The appearance and the characters of this *bc*-plane modulation structure were very similar to that found in the hole-rich (also oxygen-rich) regions of the phase-separated Cu-doped $La_2CuO_{4+\delta}$.[41] Similar to the previous conclusion,[41] the modulation structure we observed was an indication of either oxygen ordering or charge ordering. Our EELS measurements on the Cu-rich sample revealed that electron beam irradiation decreases local hole-density probably by removing some interstitial oxygen atoms.[41] The notable effect of the electron beam irradiation on the modulation structure in the heavily oxygenated $La_2CuO_{4+\delta}$ implied that the modulation structure has a strong doping dependence. With the decrease of the excess interstitial oxygen, the modulation period became shorter, i.e., the modulating planes became closer. In Fig. 6, we show two real-space diagrams of the modulation structures with a long and a short modulation period. Comparing the results of this study to that of $La_2CuO_{4.09}$ reported by Lagueyte *et al.*, the doping dependance was further confirmed. Lagueyte *et al.* reported a similar ordering structure with a vector of $0.22\mathbf{a}^*+0.32\mathbf{c}^*$ (~21 Å) in $La_2CuO_{4.09}$ at ~100 K, while in $La_2CuO_{4.12}$ we observed a modulation vector as $0.18\mathbf{b}^*+(0.26 \sim 0.28)\mathbf{c}^*$ with a longer period of ~25.5 Å. The dependence of this kind of modulation on the doping density was contradictory to the ordering of interstitial oxygen ions. In the mode of interstitial oxygen ordering, decreasing doping level necessarily means a longer modulation period. Recent neutron scattering experiments have revealed the staging behavior of the excess oxygen in $La_2CuO_{4+\delta}$ ($\delta \sim 0.09-0.1$). Excess oxygen atoms tend to form modulation structure along *c* axis, and the modulation period is *n* times the spacing between two CuO_2 layers, i.e., half of the *c* axis lattice constant. In addition, the modulation vector changed quickly under electron irradiation and even at very low temperature. These observations exclude the model of oxygen ordering. On the other side, Tranquada *et al.* reported a three-

TABLE I. Relative intensities of three superlattice reflections at five temperatures ($\mathbf{q}_0=0.18\mathbf{b}^*+0.26\mathbf{c}^*, \mathbf{q}_1=0.14\mathbf{a}^*+0.27\mathbf{b}^*+0.43\mathbf{c}^*, \mathbf{q}_3=\mathbf{a}^*/6+\mathbf{b}^*/3+\mathbf{c}^*/2$).

	100 K	140 K	180 K	220 K	260 K	300 K
$\mathbf{q}_0$	>90%	<10%	~0	~0	~0	~0
$\mathbf{q}_1$	<10%	>60%	~40%	~20%	<20%	<10%
$\mathbf{q}_2$	<10%	~30%	~60%	~80%	>80%	>90%

dimensional (3D) ordering of interstitial oxygens with similar vectors to this study.[44] In addition, it will be shown in Sec. III C that the superlattice reflection probably from oxygen stage was very weak, which may indicate that only a small part of interstitial oxygen form the stage structure along c axis. The distribution of the main part of the interstitial oxygen increases the possibility that the bc-plane modulation is due to the oxygen ordering. The definite determination of the nature of the modulation demands the real space information, such as high resolution electron microscopy. But the considerable TEM sample drift at low temperature limited the employment of this technique.

In our opinion, the interstitial oxygen ions which introduce the excess holes may situate at modulating sites. When the charge distribution starts to develop into a certain ordered pattern, it will introduce an accompanying pattern of lattice displacement. This ordered displacement field will in turn produce favorite modulating sites for the interstitial oxygen ions, i.e., charge ordering induces interstitial oxygen ordering. It must be pointed out, however, that although the charge and oxygen ion orderings are related via the tilting of the lattice, the interstitial oxygen ions and charges on the CuO_2 plane are not stuck together. When the favorite modulating sites for the interstitial oxygen ions are completely occupied, strong diffraction effects or superlattice reflections are then expected from the ordered oxygen ions. However, if the local density of the doping oxygen is not high enough, no oxygen ion ordering will be produced. The superlattice diffracted beam intensities are then resulted mainly from the combined effects of ordered charge distribution[34] and associated lattice displacement field. It is in general not possible or sensible to separate contributions from charge ordering and oxygen ion ordering, but the main idea is that the ordering is driven by the charge. Relative intensities of three main modulation superlattice reflection at different temperature is summarized in Table. I.

B. *ab*-plane modulation

Superlattice reflections have also been found in the [001] SAED patterns. At both RT and 100 K, we observed similar patterns as shown in Fig. 7 in which around each fundamental Bragg reflection four pairs of weak but well defined superlattice reflections can be found. The wave vector is measured to be $\mathbf{a}^*/6\pm\mathbf{b}^*/2$ with a period of ~10 Å. Due to the nonexistence of the superlattice reflections such as (100) and (010) expected from a two- or three-dimensional modulation, we conclude that these *ab*-plane modulation superlattice reflections result also from domains of one-dimensional modulations. A striking character of these modulation is that they are not sensitive to temperature and electron irradiation. At RT and ~100 K, we observed the same modulation vector. Moreover, 2-h irradiation under weak electron beam did not change the modulation noticeably. In addition, the intensities of the superlattice reflections were weaker than that found in for *bc*-plane modulation at ~100 K.

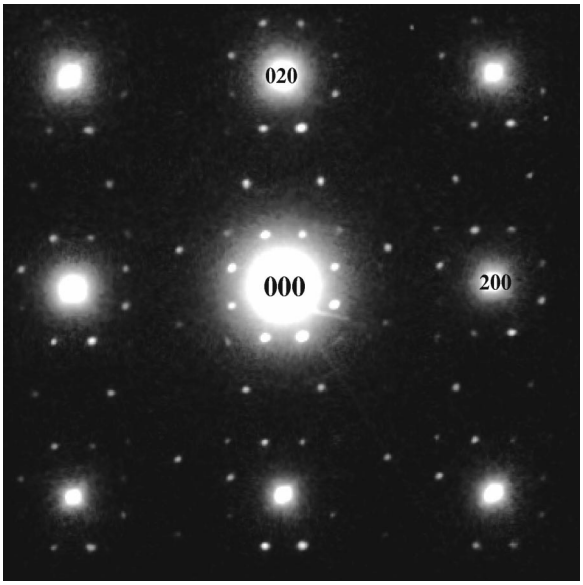

FIG. 7. [001] SAED pattern recorded from a heavily oxygen-doped $La_2CuO_{4+\delta}$ sample.

In all SAED patterns obtained along [110] and [130] zone axes from those regions with *bc*-plane modulation, the observed superlattice reflections are obviously elongated. However, the superlattice reflections observed in [001] SAED pattern were very sharp and well defined, and were not elongated. In addition, the superlattice reflections around (000) and other low order main Bragg reflections were stronger than those around the high order main Bragg reflections, and the measured $\mathbf{a}^*$ and $\mathbf{b}^*$ components were not correspondent to those of the *bc*-plane modulation structure. It may therefore be concluded that superlattice reflections found in [001] SAED pattern are not the projection of the *bc*-plane modulation superlattice reflections, instead they are a manifestation of a kind of ordering structure whose modulation direction lies in the *ab* plane.

This *ab*-plane modulation is very similar to the charge ordering reported in $La_{2-x}Sr_xNiO_4$ by Chen *et al.*[25] In $La_{2-x}Sr_xNiO_4$, these authors found a kind of modulation structure with $\mathbf{q}=\mathbf{a}^*\pm\delta\mathbf{b}^*$, for $0.075\leqslant x\leqslant 0.4$ (the hole density $p=x$), $\delta\approx 1/3$, and $\mathbf{q}\approx\mathbf{a}^*\pm\mathbf{b}^*/3$. In the present study, the hole density was estimated to be $p\approx 0.175$,[45,46] which is of the same order as the sample used by Chen *et al.* An interesting relationship is that the modulation vector in $La_2CuO_{4.12}$ is just one half of that found in $La_{2-x}Sr_xNiO_4$ with similar hole density, i.e., the modulation direction is the same, but the period of the modulation is doubled. The notable feature of the modulation in $La_{2-x}Sr_xNiO_4$ is that with the increase of the hole density (by increasing x or adding interstitial oxygen), δ decreases, i.e., the period is length-

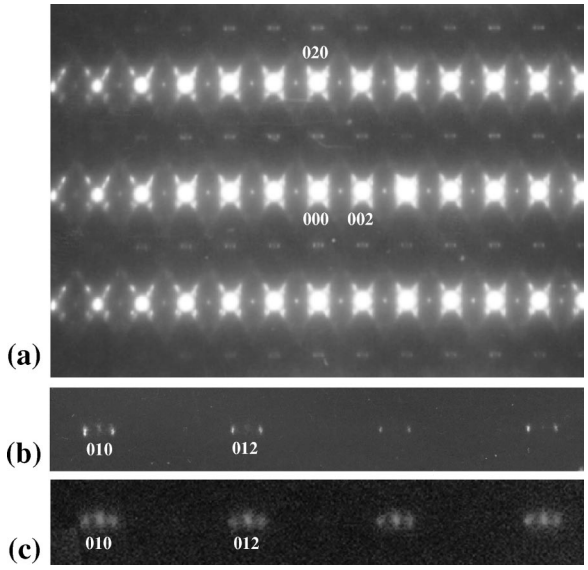

FIG. 8. (a) [100] SAED pattern from a region with the interstitial oxygen ordering. (b) Partially magnified pattern of (a). (c) Partially magnified [100] SAED pattern from the same region as (a) and (b) after long-time irradiation.

ened. This corresponds to the doping dependence of the above bc-plane modulation, and might be a universal mark of the static charge ordering found by electron diffraction in doped antiferromagnets. According to Chen *et al.*, the ab-plane charge order in $La_{2-x}Sr_xNiO_4$ appeared below 220 K, and the modulation vector remained unchangeable down to 15 K. In addition, the modulation vector did not change within a wide doping range. These are also correspondent to the characters of the ab-plane modulation in this study, which is not sensitive to the temperature and the electron irradiation. In $La_{2-x}Sr_xNiO_4$, only the first order superlattice reflections are observable, while in $La_2CuO_{4.12}$, it is not difficult to recognize up to third order superlattice reflections. This indicates that in the charge ordering in doped antiferromagnets, the hole concentrated layers in a system with mobile holes introduced by interstitial oxygen are much better defined than that formed by holes introduced by immobile alkaline earth cations.

C. Modulation structure along *c* axis

In some areas of the sample, superlattice reflections indicating an ordering structure along *c* axis was found in SAED patterns recorded at ~100 K. Figure 8(a) shows a [100] SAED pattern recorded at ~100 K from such an area and the portion containing weak (01l) reflections is magnified in Fig. 8(b). In addition to the (01l) weak reflections, two additional reflections appeared around each such main reflection and their intensities exceeded that of the main (01l) reflections [see Fig. 8(b)]. Other superlattice reflections are very weak and their corresponding vectors are very short, and may not be identified easily around the strong main Bragg reflections. The modulation wave vector around the main weak (01l) reflections was measured to be $\mathbf{q} = 0.193\mathbf{c}^* \approx \mathbf{c}^*/5.2$. Compared with the bc- and ab-plane modulation discussed in previous sections, this ordering structure along *c* axis exhibited some different features. First, it cannot be observed in all oxygen-rich regions. Second, its period (~70 Å) was much longer. In addition, only the first order superlattice reflections may be observed, suggesting an essentially sinusoidal character.

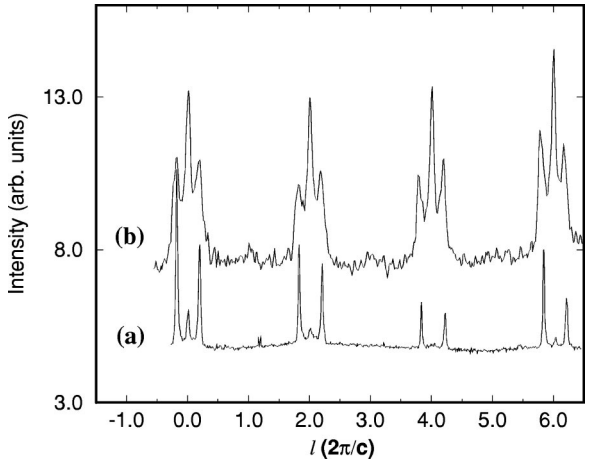

FIG. 9. Intensity profiles along the line containing (01l) reflections of Figs. 8(b) (line a) and 8(c) (line b).

The sample temperature was found to play a crucial influence on this ordering structure. The superlattice reflections only became observable at temperatures below 200 K. On the other hand, the electron irradiation also changed the ordering significantly. In Fig. 8(c), we show a portion of a [100] SAED pattern recorded from the same region as Fig. 8(a) but after a long-time irradiation. The (01l) reflections became stronger and the superlattice reflections became weaker and blurred considerably. Figure 9 shows the intensity profiles along (01l) reflections, and the lines marked *a* and *b* correspond to Figs. 8(b) and 8(c), respectively. It should be noted that the superlattice reflections are broadened and the two superlattice reflections are not centered on the (01l) peaks, especially when l increases.

In previous TEM studies on $La_2CuO_{4+\delta}$ and $La_2NiO_{4+\delta}$, no modulation along *c* axis was reported. Considering its agreement with the results of neutron diffraction, we suggest that the superlattice reflections along *c* axis result from interstitial oxygen staging. It has been pointed out that the staging of the interstitial oxygen in $La_2CuO_{4+\delta}$ and $La_2NiO_{4+\delta}$ manifests itself through the antiphase boundarylike tilt pattern of the CuO_6 and NiO_6 octahedra (and the concomitant displacements of the La ions). The period of the tilt pattern is twice that of the spacing between the intercalant layers.[31] In this study, the vector of $0.193\mathbf{c}^*$ can be understood by using a random mixture of stage 5 and stage 6. Our results also indicated that the staging of the interstitial oxygen was not a universal phenomenon in the oxygen doped $La_2CuO_{4+\delta}$ samples. Though it was shown that the interstitial oxygen in $Bmab$ $La_2CuO_{4+\delta}$ and $La_2NiO_{4+\delta}$ had a tendency to form staging structure along *c* axis, it was difficult for the interstitial oxygen to form a uniform staging structure corresponding to the lowest energy configuration due to the slow diffusion of the intercalant especially when the interlayer diffusion was involved.

Electron irradiation may decrease the density of the interstitial oxygen atoms. In those regions where much loss of the interstitial oxygen occurred, the space group would change from $Fmmm$ to $Bmab$, so $(01l)$ reflections became stronger. On the other hand, the irradiation would disorder the staging structure and cause the existence of more phases with different staging numbers, this would lead to the bluring and broadening of the superlattice reflections. The oxygen staging only exists in the oxygen-rich phases with $Fmmm$ space group symmetry, and the $(01l)$ reflections come from the oxygen-poor phases with $Bmab$ space group. The difference in c lattice parameters for the Bmab phase and the O-ordering phases would cause the two superlattice reflections not centered on the $Bmab$ $(01l)$ peak, which was also reported by Xiong *et al.* by using neutron diffraction.[29]

IV. CONCLUSION

In this study, several types of modulation structures have been found to exist in a heavily oxygenated $La_2CuO_{4.12}$ sample by the technique of electron diffraction, and the effects of temperature and the electron irradiation on the modulation structure have been investigated. In this heavily oxygenated $La_2CuO_{4+\delta}$ sample, modulation wave vectors were observed in several principal zone axes and found to lie either in bc or ab plane. The bc-plane modulation structure exhibited obvious temperature and doping dependence. Low temperature and high hole density were found to enhance the modulation superlattice reflections and favor a longer period, in contrast to the modulation structure expected from the ordering of oxygen or other ions presented in the sample but in agreement with that expected for a charge ordering structure. The appearance of up to third harmonics of both the bc- and ab-plane modulations suggests that the modulating layers were much narrower and well defined than that found in $La_{2-x}Sr_xNiO_4$. In some areas of our oxygenated samples, superlattice reflections resulting from the ordering of doped oxygen along c axis were also observed.

ACKNOWLEDGMENTS

This work was supported by National Natural Science foundation of China, and the Chinese Academy of Sciences.

*Corresponding author. Email address: lmpeng @lmplab.blem.ac.cn

[1] J.D. Jorgensen, B. Dabrowski, Shiyou Pei, D.G. Hinks, L. Soderholm, B. Morosin, J.E. Schirber, E.L. Venturini, and D.S. Ginley, Phys. Rev. B **38**, 11 337 (1988).

[2] *International School of Solid State Physics, Proceedings of the 3rd Workshop: Phase Separation in Cuprate Superconductors*, edited by K.A. Müller and G. Benedek (World Scientific, Singapore, 1993).

[3] R.K. Kremer, V. Hizhnyakov, E. Sigmund, A. Simon, and K.A. Müller, Z. Phys. B: Condens. Matter **91**, 169 (1993).

[4] V.J. Emery, S.A. Kivelson, and H.Q. Lin, Phys. Rev. Lett. **64**, 475 (1990).

[5] V.J. Emery and S.A. Kivelson, Physica C **209**, 597 (1993).

[6] O. Zachar, S.A. Kivelson, and V.J. Emery, Phys. Rev. B **57**, 1422 (1998).

[7] B. Dabrowski, D.G. Hinks, J.D. Jorgensen, and D.R. Richards, *High-Temperature Superconductors: Relationship Between Properties, Structure and Solid State Chemistry* (Materials Research Society, Pittsburgh, 1989), p. 69.

[8] B. Dabrowski, J.D. Jorgensen, D.G. Hinks, S. Pei, D.R. Richards, H.B. Vanfleet, and D.L. Decker, Physica C **162-164**, 99 (1989).

[9] P.G. Radaelli, J.D. Jorgensen, A.J. Schultz, B.A. Hunter, J.L. Wagner, F.C. Chou, and D.C. Johnston, Phys. Rev. B **48**, 499 (1993).

[10] J.D. Jorgensen, B. Dabrowski, S. Pei, D.R. Richards, and D.G. Hinks, Phys. Rev. B **40**, 2187 (1989).

[11] C. Chaillout, S.-W. Cheong, Z. Fisk, M.S. Lehmann, M. Marezio, B. Morosin, and J.E. Schirber, Physica C **158**, 183 (1989).

[12] V.J. Emery, S.A. Kivelson, and J.M. Tranquada, cond-mat/9907228 (unpublished), and references therein.

[13] V.J. Emery and S.A. Kivelson, Physica C **263**, 44 (1996).

[14] J.M. Tranquada, B.J. Sternlieb, J.D. Axe, Y. Nakamura, and S. Uchida, Nature (London) **375**, 561 (1995).

[15] B.O. Wells, Y.S. Lee, M.A. Kastner, R.J. Christianson, R.J. Birgeneau, K. Yamada, Y. Endoh, and G. Shirane, Science **277**, 1067 (1997).

[16] B.G. Levi, Phys. Today **51** (6), 19 (1998).

[17] R.F. Service, Science **283**, 1106 (1999).

[18] P.C. Hammel, A.P. Reyes, S-W. Cheong, Z. Fisk, and J.E. Schirber, Phys. Rev. Lett. **71**, 440 (1993).

[19] A.W. Hunt, P.M. Singer, K.R. Thurber, and T. Imai, Phys. Rev. Lett. **82**, 4300 (1999).

[20] A. Bianconi, N.L. Saini, A. Lanzara, M. Missori, T. Rossetti, H. Oyanagi, H. Yamaguchi, O. Oka, and T. Ito, Phys. Rev. Lett. **76**, 3412 (1996).

[21] A. Lanzara, N.L. Saini, A. Bianconi, F.C. Chou, and D.C. Johnston, Physica C **296**, 7 (1998).

[22] A. Lanzara, N.L. Saini, A. Bianconi, J.L. Hazemann, Y. Soldo, F.C. Chou, and D.C. Johnston, Phys. Rev. B **55**, 9120 (1997).

[23] M.V. Zimmermann, A. Vigliante, T. Niemöller, N. Ichikawa, T. Frello, J. Madsen, P. Wochner, S. Uchida, N.H. Andersen, J.M. Tranquanda, D. Gibbs, and R. Schneider, Europhys. Lett. **41**, 629 (1998).

[24] Z.J. Zhou, P. Bogdanov, S.A. Kellar, T. Noda, H. Eisaki, S. Uchida, Z. Hussain, and Z.-X. Shen, Science **286**, 268 (1999).

[25] C.H. Chen, S-W. Cheong, and A.S. Cooper, Phys. Rev. Lett. **71**, 2461 (1993).

[26] C.H. Chen, S-W. Cheong, and H.Y. Hwang, J. Appl. Phys. **81**, 4326 (1997).

[27] S. Mori, C.H. Chen, and S-W. Cheong, Nature (London) **392**, 473 (1998).

[28] P. Blakeslee, R.J. Birgeneau, F.C. Chou, R. Christianson, M.A. Kastner, Y.S. Lee, and B.O. Wells, Phys. Rev. B **57**, 13 915 (1998).

[29] X. Xiong, P. Wochner, S.C. Moss, Y. Cao, K. Koga, and M. Fujita, Phys. Rev. Lett. **76**, 2997 (1996).

[30] B.O. Wells, R.J. Birgeneau, F.c. Chou, Y. Endoh, D.C. Johnston, M.A. Kastner, Y.S. Lee, G. Shirane, J.M. Tranquada, and K. Yamada, Z. Phys. B: Condens. Matter **100**, 535 (1996).

[31] J.M. Tranquada, Y. Kong, J.E. Lorenzo, D.J. Buttrey, D.E. Rice, and V. Sachan, Phys. Rev. B **50**, 6340 (1994).
[32] P. Wochner, X. Xiong, and S.C. Moss, J. Supercond. **10**, 367 (1997).
[33] L. Wu, Y. Zhu, and J. Tafto, Micron **30**, 357 (1999).
[34] L.-M. Peng, Z.F. Dong, X.L. Dong, B.R. Zhao, X.F. Duan, and Z.X. Zhao, Micron **31**, 551 (2000).
[35] E. Takayama-Muromachi, T. Sasaki, and Y. Matsui, Physica C **207**, 97 (1993).
[36] N. Lagueyte, F. Weill, A. Wattiaux, and J.C. Grenier, Eur. J. Solid State Inorg. Chem. **30**, 857 (1993).
[37] L.C. Otero-Diaz, A.R. Landa, F. Fernandez, R. Saez-Puche, R. Withers, and B.G. Hyde, J. Solid State Chem. **97**, 443 (1992).
[38] A. Demourgues, F. Weill, J.C. Grenier, A. Wattiaux, and M. Pouchard, Physica C **192**, 425 (1992).
[39] Z. Hiroi, T. Obata, M. Takano, and Y. Bando, Phys. Rev. B **41**, 11 665 (1990).
[40] L.-M. Peng, M. Gao, Z.F. Dong, X.L. Dong, P.R. Zhao, and Z.X. Zhao, Phys. Rev. B **62**, 189 (2000).
[41] M. Gao, L.-M. Peng, X.L. Dong, B.R. Zhao, G.D. Liu, and Z.X. Zhao, Phys. Rev. B **62**, 5413 (2000).
[42] E. Takayama-Muromachi and A. Narrotsky, Physica C **218**, 164 (1993).
[43] G.D. Liu, M. Gao, G.C. Che, Z.X. Zhao, L. Chen, C. Dong, F. Wu, Y.M. Ni, H. Chen, and L.-M. Peng, Supercond. Sci. Technol. **14**, 398 (2001).
[44] J.M. Tranquada, J.E. Lorenzo, D.J. Buttrey, and V. Sachan, Phys. Rev. B **52**, 3581 (1995).
[45] Z.G. Li, H.H. Feng, Z.Y. Yang, A. Hamed, S.T. Ting, P.H. Hor, S. Bhavaraju, J.F. DiCarlo, and A.J. Jacobson, Phys. Rev. Lett. **77**, 5413 (1996).
[46] X.L. Dong, Z.F. Dong, B.R. Zhao, Z.X. Zhao, X.F. Duan, L.-M. Peng, W.W. Huang, B. Xu, Y.Z. Zhang, S.Q. Guo, L.H. Zhao, and L. Li, Phys. Rev. Lett. **80**, 2701 (1998).